MOLECULAR DYNAMICS SIMULATION OF DOUBLE-WALLED CARBON NANOTUBE VIBRATIONS: COMPARISON WITH CONTINUUM ELASTIC THERORIES

S. S. Amin *

Department of Mechanical and Aerospace Engineering
Tokyo Institute of Technology
152-8552, Tokyo, Japan

H. Dalir **

Department of Mechano-Micro Engineering
Tokyo Institute of Technology
226-8503, Tokyo, Japan

A. Farshidianfar ***

Department of Mechanical Engineering
Ferdowsi University of Mashhad
Mashhad, Iran

ABSTRACT

Double-walled carbon nanotubes (DWNTs) are expected to be useful as elements in improving conventional polymer-based fibers and films. An extensive molecular dynamics simulation and continuum analyses are carried out to estimate the influence of matrix stiffness and the intertube radial displacements on free vibration of an individual DWNT. The effects of nanotube length and chirality are also taken into account. The continuum analyses are based on both Euler-Bernoulli and Timoshenko beam theories which considers shear deformation and rotary inertia and for both concentric and non-concentric assumptions considering intertube radial displacements and the related internal degrees of freedom. New intertube resonant frequencies are calculated. Detailed results are demonstrated for the dependence of resonant frequencies on the matrix stiffness. The results indicate that internal radial displacement and surrounding matrix stiffness could substantially affect resonant frequencies especially for longer double-walled carbon nanotubes of larger innermost radius at higher resonant frequencies, and thus the latter does not keep the otherwise concentric structure at ultrahigh frequencies.

Keywords : Carbon nanotubes, Molecular dynamics, Continuum models, Vibrational analysis.

1. INTRODUCTION

Carbon nanotubes (CNTs) are promising materials for the creation of novel nanodevices [1,2]. From an mechanical point of view, CNTs provide superfibers for nanocomposites [3,4]. In addition, CNTs are well known for their excellent rigidity, superior to that of steel and any other metal. Such superior properties are suitable for use in fabricating nanometre-scale electromechanical systems (NEMS). On the other hand, a double-walled carbon nanotube (DWNT) is usually produced in conventional synthesis processes. The DWNT is suitable for creating a nano-mechanical element such as superfibers for nanocomposites. The dynamics between the inner and outer tubes are important to the design and the manipulation of DWNTs in actual experiments.

Recently, solid mechanics with continuum elastic models have been widely and successfully used to study mechanical behavior of CNTs, such as static deflection [5], buckling [6-8], thermal vibration [9,10], resonant frequencies and modes [11-15]. Moreover, interest in DWNTs is rising due to the progress in large-scale synthesis of DWNTs [16,17]. In many proposed applications and designs, however, CNTs are often embedded in another elastic medium [18], or constrained periodically [19], or of smaller aspect ratios [20]. Quantitative theoretical studies have also been carried out for DWNTs. An artificial DWNT gigahertz oscillator has been theoretically investigated by Zheng and Jiang using a static continuous model [21] and by Legoas *et al.* using a molecular dynamics (MD) simulation [22].

In this paper, a quantitative study of vibration of DWNTs by numerical simulation is reported. To reduce the calculation cost, a classical molecular dynamics method is applied to analyze interaction between tubes. The calculation is carried out for both molecular dynamics and continuum mechanics approaches.

2. MOLECULAR DYNAMICS SIMULATION

2.1 Interatomic Potential

* Medi???? **???, corresponding author *** Ph????

In MD simulations, the potential used in the model is the key to describing the system realistically. We apply a Tersoff-Brenner (TB) potential [23] to describe a covalently bonded pair of atoms. The TB potential has been developed to describe bond forming and breaking during chemical vapor deposition, so the potential has good transferability to various carbon structures. On the other hand, we apply the Lennard-Jones potential in Eq. (1) to a non-covalent pair of atoms as

$$u_{LJ}(r_{ij}) = 4\varepsilon\left\{-\left(\frac{\sigma}{r_{ij}}\right)^{6}+\left(\frac{\sigma}{r_{ij}}\right)^{12}\right\}, \qquad (1)$$

where, r_{ij} is the distance between atoms i and j, and $u_{LJ}(r_{ij})$ is the Lennard-Jones potential between them. We use the parameters ε, σ which have been given by Gilifalco *et al.* for the graphene-graphene interaction [24]. The van der Waals interaction for the entire DWNT is evaluated by summing $u_{LJ}(r_{ij})$ over all inter-tube i, j-pairs:

$$U_{VDW} = \sum_{i\neq j} u_{LJ}(r_{ij}) . \qquad (2)$$

2.2 Initial and Boundary Conditions

The DWNT model is simply constructed by placing two SWNT models coaxially. In order to examine the effects of length-to-radius aspect ratio and chiralities on the fundamental vibrational frequency, we perform the analysis for three different DWNTs, (5, 5)/(10, 10), (5, 5)/(17, 0) and (5, 5)/(15, 4), with the same inner tube structure and different outer tube chirality owning same diameter. For each simulation, the canonical (NVT) ensemble with a fixed temperature (300K) is first used to equilibrate the structure and both the center-of-mass velocity and total angular momentum of each tube are equal to zero. The C-end atoms of the inner and outer tubes within 5 $\mathring{A}$ from the edge are fixed in all simulation steps. 100,000MD equilibration steps (with a fixed time step 1fs) are carried out until the system has reached ambient temperature, 300K. The displacement histories of carbon atoms are recorded in the next 1ns, from which the lateral vibrational frequencies are calculated by using fast Fourier transform (FFT).

Since MD analyses yield explicit information, in order to overcome its length- and time-scale limits, simple continuum-based models are needed to closely duplicate the atomistic simulation. Yet it is unclear whether there exists a synergism between MD and continuum modeling on the dynamic behavior of DWNTs.

3. CNTs CONTINUUM-BASED MODELS

Many researchers have shown that classic elastic-Euler beam offers a reliable model for overall mechanical deformation of CNTs [6,9-11,20]. In particular, because elastic-Euler-beam models give simple general formulas in many important cases, such as resonant frequencies and modes, they have the potential to identify the key parameters, explain or predict new physical phenomena, and stimulate and guide further experiments and molecular dynamics simulations. So far, most of the elastic-Euler-beam models used for CNTs are based on the classic single Euler-beam model [6]. The single elastic-Euler-beam model assumes that all nested individual tubes of a MWNT remain coaxial during deformation and thus can be described by a single deflection curve and it also neglects the effects of shear deformation and rotary inertia. As will be shown by the current work, rotary inertia and shear deformation, incorporated by Timoshenko-beam model, do have a substantial effect on carbon nanotube-reinforced composite's frequency analysis results. Therefore, depending on the stiffness of the matrix, an appropriate theory for nanotube-reinforced composite's frequency analysis should be chosen.

Since the inner and outer diameters of three different DWNTs, (5, 5)/(10, 10), (5, 5)/(17, 0) and (5, 5)/(15, 4), considered in this paper are almost the same, a double-elastic beam model developed by both Euler-Bernoulli and Timoshenko theories is considered, in which each of the nested, originally concentric nanotubes of a DWNT is described as an individual elastic beam, and the deflections of two nested tubes are coupled through the van der Waals interaction between two adjacent tubes.

3.1 Euler-Bernoulli Model

3.1.1 Single-Elastic Beam Model

Since the single-beam model assumes that two originally concentric tubes of a DWNT remain coaxial during vibration and thus can be described by a single deflection curve as

$$EI\frac{\partial^4 w(x,\,t)}{\partial x^4}+\rho A\frac{\partial^2 w(x,\,t)}{\partial t^2} = -kw\,(x,\,t)\,, \qquad (3)$$

where $I = I_1 + I_2$ and $A = A_1 + A_2$ are the total moment of inertia and cross-sectional area related to the inner (A_1, I_1) and outer DWNT tubes (A_2, I_2). It is assumed the two tubes have the same Young's modulus E = 1 Tpa and shear modulus G = 0.373Tpa (with Poisson ratio υ = 0.34), with the effective thickness of single-walled nanotubes 0.35nm and the mass density of ρ = 1.3g/cm^3. $-kw(x, t)$ is the Winkler-like model of the pressure per unit axial length acting on the outermost tube due to the surrounding elastic matrix [25,26] and k is a constant determined by the material constants of the elastic medium, the outermost diameter of the embedded MWNT, and the wave-length of vibrational modes. This simple model is especially relevant if the constant k is allowed to be dependent on the wave-length [25,26]. For example, for an elastic medium (such as polymers) of a Young's modulus of 2GPa [27], the dependency of k on the mode number n has been denoted in [25], Eqs. (53-54). In our present analysis, the parameter ($n\pi d/L$), where n, d and L are mode number, outermost diameter and length of the DWNT respectively, is be-

Molecular Dynamics Simulation of Double-walled Carbon nanotube Vibrations: comparison with continuum elastic therories

Sara Shayan Amin[1], Hamid Dalir[2]

and Anooshirvan Farshidianfar[3]

[1]Department of Mechanical and Aerospace Engineering,

Tokyo Institute of Technology, 152-8552, Tokyo, Japan.

[2]Department of Mechano-Micro Engineering,

Tokyo Institute of Technology, 226-8503, Tokyo, Japan.

[3]Department of Mechanical Engineering,

Ferdowsi University of Mashhad, Mashhad, Iran.

Corresponding author. Phone/fax: +81-45-924-5088.
E-mail address: dalir.h.aa@m.titech.ac.jp (H. Dalir).

Abstract

Double-walled carbon nanotubes (DWNTs) are expected to be useful as elements in improving conventional polymer-based fibers and films. An extensive molecular dynamics simulation and continuum analyses are carried out to estimate the influence of matrix stiffness and the intertube radial displacements on free vibration of an individual DWNT. The effects of nanotube length and chirality are also taken into account. The continuum analyses are based on both Euler-Bernoulli and Timoshenko beam theories which considers shear deformation and rotary inertia and for both concentric and non-concentric assumptions considering intertube radial displacements and the related internal degrees of freedom. New intertube resonant frequencies are calculated. Detailed results are demonstrated for the dependence of resonant frequencies on the matrix stiffness. The results indicate that internal radial displacement and surrounding matrix stiffness could substantially affect resonant frequencies especially for longer double-walled carbon nanotubes of larger innermost radius at higher resonant frequencies, and thus the latter does not keep the otherwise concentric structure at ultrahigh frequencies.

Keywords: Carbon nanotubes; Molecular dynamics; Continuum models; Vibrational analysis

1. Introduction

Carbon nanotubes (CNTs) are promising materials for the creation of novel nanodevices [1,2]. From an mechanical point of view, CNTs provide superfibers for nanocomposites [3,4]. In addition, CNTs are well known for their excellent rigidity, superior to that of steel and any other metal. Such superior properties are suitable for use in fabricating nanometre-scale electromechanical systems (NEMS). On the other hand, a double-walled carbon nanotube (DWNT) is usually produced in conventional synthesis processes. The DWNT is suitable for creating a nano-mechanical element such as superfibers for nanocomposites. The dynamics between the inner and outer tubes are important to the design and the manipulation of DWNTs in actual experiments.

Recently, solid mechanics with continuum elastic models have been widely and successfully used to study mechanical behavior of CNTs, such as static deflection [5], buckling [6-8], thermal vibration [9,10], resonant frequencies and modes [11-15]. Moreover, interest in DWNTs is rising due to the progress in large-scale synthesis of DWNTs [16,17]. In many proposed applications and designs, however, CNTs are often embedded in another elastic medium [18], or constrained periodically [19], or of smaller aspect ratios [20]. Quantitative theoretical studies have also been carried out for DWNTs. An artificial DWNT gigahertz oscillator has been theoretically investigated by Zheng and Jiang using a static continuous

model [21] and by Legoas *et al.* using a molecular dynamics (MD) simulation [22].

In this paper, a quantitative study of vibration of DWNTs by numerical simulation is reported. To reduce the calculation cost, a classical molecular dynamics method is applied to analyze interaction between tubes. The calculation is carried out for both molecular dynamics and continuum mechanics approaches.

2. Molecular dynamics simulation

2.1 Interatomic potential

In MD simulations, the potential used in the model is the key to describing the system realistically. We apply a Tersoff–Brenner (TB) potential [23] to describe a covalently bonded pair of atoms. The TB potential has been developed to describe bond forming and breaking during chemical vapor deposition, so the potential has good transferability to various carbon structures. On the other hand, we apply the Lennard-Jones potential in Equation (1) to a non-covalent pair of atoms as

$$u_{LJ}\left(r_{ij}\right)=4\varepsilon\left\{-\left(\frac{\sigma}{r_{ij}}\right)^{6}+\left(\frac{\sigma}{r_{ij}}\right)^{12}\right\}, \tag{1}$$

where, r_{ij} is the distance between atoms i and j, and $u_{LJ}\left(r_{ij}\right)$ is the Lennard–Jones potential between them. We use the parameters ε , σ which have been given by Gilifalco *et al.* for the graphene-graphene

interaction [24]. The van der Waals interaction for the entire DWNT is evaluated by summing $u_{LJ}\left(r_{ij}\right)$ over all inter-tube i, j-pairs:

$$U_{VDW} = \sum_{i \neq j} u_{LJ}\left(r_{ij}\right). \tag{2}$$

2.2 Initial and boundary conditions

The DWNT model is simply constructed by placing two SWNT models coaxially. In order to examine the effects of length-to-radius aspect ratio and chiralities on the fundamental vibrational frequency, we perform the analysis for three different DWNTs, (5,5)/(10,10), (5,5)/(17,0) and (5,5)/(15,4), with the same inner tube structure and different outer tube chirality owning same diameter. For each simulation, the canonical (NVT) ensemble with a fixed temperature (300 K) is first used to equilibrate the structure and both the center-of-mass velocity and total angular momentum of each tube are equal to zero. The C-end atoms of the inner and outer tubes within $5\,\text{Å}$ from the edge are fixed in all simulation steps. 100,000 MD equilibration steps (with a fixed time step 1 fs) are carried out until the system has reached ambient temperature, 300 K. The displacement histories of carbon atoms are recorded in the next 1 ns, from which the lateral vibrational frequencies are calculated by using fast Fourier transform (FFT).

Since MD analyses yield explicit information, in order to overcome its length- and time-scale limits, simple continuum-based models are needed

to closely duplicate the atomistic simulation. Yet it is unclear whether there exists a synergism between MD and continuum modeling on the dynamic behavior of DWNTs.

3. CNTs continuum-based models

Many researchers have shown that classic elastic-Euler beam offers a reliable model for overall mechanical deformation of CNTs [6, 9-11, 20]. In particular, because elastic-Euler-beam models give simple general formulas in many important cases, such as resonant frequencies and modes, they have the potential to identify the key parameters, explain or predict new physical phenomena, and stimulate and guide further experiments and molecular dynamics simulations. So far, most of the elastic-Euler-beam models used for CNTs are based on the classic single Euler-beam model [6]. The single elastic-Euler-beam model assumes that all nested individual tubes of a MWNT remain coaxial during deformation and thus can be described by a single deflection curve and it also neglects the effects of shear deformation and rotary inertia. As will be shown by the current work, rotary inertia and shear deformation, incorporated by Timoshenko-beam model, do have a substantial effect on carbon nanotube-reinforced composite's frequency analysis results. Therefore, depending on the stiffness of the matrix, an appropriate theory for nanotube-reinforced composite's frequency analysis should be chosen.

Since the inner and outer diameters of three different DWNTs, (5,5)/(10,10), (5,5)/(17,0) and (5,5)/(15,4), considered in this paper are almost the same, a double-elastic beam model developed by both Euler-Bernoulli and Timoshenko theories is considered, in which each of the nested, originally concentric nanotubes of a DWNT is described as an individual elastic beam, and the deflections of two nested tubes are coupled through the van der Waals interaction between two adjacent tubes.

3.1. Euler-Bernoulli model

3.1.1 Single-elastic beam model

Since the single-beam model assumes that two originally concentric tubes of a DWNT remain coaxial during vibration and thus can be described by a single deflection curve as

$$EI\frac{\partial^4 w(x,t)}{\partial x^4}+\rho A\frac{\partial^2 w(x,t)}{\partial t^2}=-kw(x,t), \tag{3}$$

where $I=I_1+I_2$ and $A=A_1+A_2$ are the total moment of inertia and cross-sectional area related to the inner (A_1, I_1) and outer DWNT tubes (A_2, I_2). It is assumed the two tubes have the same Young's modulus E=1 Tpa and shear modulus G=0.373 Tpa (with Poisson ratio υ=0.34), with the effective thickness of single-walled nanotubes 0.35 nm and the mass density of ρ=1.3g/cm^3. $-kw(x,t)$ is the Winkler-like model of the

pressure per unit axial length acting on the outermost tube due to the surrounding elastic matrix [25,26] and k is a constant determined by the material constants of the elastic medium, the outermost diameter of the embedded MWNT, and the wave-length of vibrational modes. This simple model is especially relevant if the constant k is allowed to be dependent on the wave-length [25,26]. For example, for an elastic medium (such as polymers) of a Young's modulus of 2 GPa [27], the dependency of k on the mode number n has been denoted in [[25], Eqs. (53-54)]. In our present analysis, the parameter ($n\pi d/L$), where n, d and L are mode number, outermost diameter and length of the DWNT respectively, is between 0.06 and 1. It can be seen that the constant k almost linearly increases with the mode number n in this range [25]. On the other hand, because k is proportional to the Young's modulus of the surrounding elastic medium, the value of k for other Young's moduli can be easily obtained by the following form

$$k(Gpa)=\left(3.125\left(\frac{n\pi d}{L}\right)+0.875\right)E(Gpa), \text{ when } 0.06\le\frac{n\pi d}{L}\le 1. \qquad (4)$$

Since both nested individual nanotubes of the DWNT have the same end boundary conditions. Thus, it can be verified that all nested tubes share the same vibrational modes $Y_n(x)=c_1\sin\lambda_n x+c_2\cos\lambda_n x+c_3\sinh\lambda_n x+c_4\cosh\lambda_n x$. The value λ_n can be determined by considering $Y_n(0)=Y_n(L)=Y_n'(0)=Y_n'(L)=0$ as the fixed

end boundary conditions. The first three λ_n values are 4.730/*L*, 7.853/*L* and 10.995/*L*. Thus, for the *n*-order vibrational mode, the frequency-equation can be obtained as,

$$\omega_n = \left(\frac{EI\lambda_n{}^4 + k}{\rho A} \right)^{1/2}. \tag{5}$$

3.1.2 Double-elastic beam model

In contrast to the previously Euler-Bernoulli coaxial modelling, by applying Equation (3) to each of the inner and outer tubes of the DWNT to demonstrate essential ideas of intertube vibration, transverse vibration of the DWNT is described by the following two equations

$$EI_1 \frac{\partial^4 w_1(x,t)}{\partial x^4} + \rho A_1 \frac{\partial^2 w_1(x,t)}{\partial t^2} = c\left(w_2(x,t) - w_1(x,t)\right), \tag{6}$$

$$EI_2 \frac{\partial^4 w_2(x,t)}{\partial x^4} + \rho A_2 \frac{\partial^2 w_2(x,t)}{\partial t^2} = -c\left(w_2(x,t) - w_1(x,t)\right) - k w_2(x,t), \tag{7}$$

where indexes 1 and 2 denote the inner and outer tube parameters of the DWNT, respectively. To prevent slippage among the tubes, the horizontal motion of carbon atoms along the tubes are restricted. Moreover, it is noticed that the deflections of the two tubes are coupled through the van der Waals intertube interaction $c\left(w_2(x,t) - w_1(x,t)\right)$, where the van der Waals interaction coefficients *c* for interaction pressure per unit axial length can be estimated based on an effective interaction width $(2R_1)$ of the tubes as [28]

$$c = \frac{200 \times (2R_1)}{0.16 d^2}, \tag{8}$$

where R_1 is the inner radius of DWNTs and d=0.142 nm [28].

Assuming that all nested tubes share the same vibrational mode $Y_n(x)$ and also considering $w_{1n}(x,t) = W_1 e^{i\omega_n t} Y_n(x)$ and $w_{2n}(x,t) = W_2 e^{i\omega_n t} Y_n(x)$, one can derive two coupled equations for two unknowns W_1 and W_2 as

$$\begin{bmatrix} EI_1 \lambda_n^{\,4} + c - \rho A_1 \omega_n^{\,2} & -c \\ -c & EI_2 \lambda_n^{\,4} + c + k - \rho A_2 \omega_n^{\,2} \end{bmatrix} \begin{bmatrix} W_1 \\ W_2 \end{bmatrix} = 0_{2\times 1}. \tag{9}$$

The two lower and upper n-order critical frequencies in contrast with the only n-order resonant frequency given by single-elastic Euler-Bernoulli beam model are determined by the condition for existence of non-zero solution of (9) in the following form

$$\begin{aligned} \omega_{n1} &= \frac{1}{\sqrt{2}} \left(\xi_n - \sqrt{\xi_n^{\,2} - 4\eta_n} \right)^{\frac{1}{2}}, \\ \omega_{n2} &= \frac{1}{\sqrt{2}} \left(\xi_n + \sqrt{\xi_n^{\,2} - 4\eta_n} \right)^{\frac{1}{2}}, \end{aligned} \tag{10}$$

where

$$\begin{aligned} \xi_n &= \frac{1}{\rho^2 A_1 A_2} \left(\left(k + c + EI_2 \lambda_n^{\,4} \right) \rho A_1 + \left(c + EI_1 \lambda_n^{\,4} \right) \rho A_2 \right) > 2\eta_n^{\,1/2}, \\ \eta_n &= \frac{1}{\rho^2 A_1 A_2} \left(E^2 I_1 I_2 \lambda_n^{\,8} + \left(EI_1 (c+k) + EI_2 c \right) \lambda_n^{\,4} + ck \right). \end{aligned} \tag{11}$$

3.2.1 Single-elastic beam model

To study the effects of shear deformation and rotary inertia on the frequency analysis in individual carbon nanotubes, one can consider Timoshenko beam equation as

$$EI\frac{\partial^4 w(x,t)}{\partial x^4}+\left(\rho A+\frac{k\rho I}{\kappa AG}\right)\frac{\partial^2 w(x,t)}{\partial t^2}+\frac{\rho^2 I}{kG}\frac{\partial^4 w(x,t)}{\partial t^4}-\frac{kEI}{\kappa AG}\frac{\partial^2 w(x,t)}{\partial x^2}$$
$$-\left(\frac{\rho EI}{\kappa G}+\rho I\right)\frac{\partial^4 w(x,t)}{\partial x^2\partial t^2}+kw(x,t)=0, \tag{12}$$

where κ for the thin-walled circular cross-sections of DWNTs defined as the cross-sectional shape factor, can be determined by [29]

$$\kappa=\frac{2(1+\upsilon)}{4+3\upsilon}. \tag{13}$$

By considering $w_n(x,t)=We^{i\omega_n t}Y_n(x)$ and $\Psi_n(x,t)=\psi e^{i\omega_n t}\Psi_n(x)$, where W and ψ represent the amplitude and slope due to bending of the DWNT, one can easily obtain

$$Y_n(x)=c_1\,cosh\,\lambda_n x+c_2\,sinh\,\lambda_n x+c_3\,cos\,\gamma_n x+c_4\,sin\,\gamma_n x, \tag{14}$$

$$\Psi_n(x)=\left(\lambda_n+\frac{\beta_n^{\,2}}{\lambda_n}\right)c_1\sinh\lambda_n x+\left(\lambda_n+\frac{\beta_n^{\,2}}{\lambda_n}\right)c_2\cosh\lambda_n x$$
$$+\left(\frac{\beta_n^{\,2}}{\gamma_n}-\gamma_n\right)c_3\sin\gamma_n x-\left(\frac{\beta_n^{\,2}}{\gamma_n}-\gamma_n\right)c_4\cos\gamma_n x, \tag{15}$$

where

$$\lambda_n^{\,2}=\frac{1}{2}\left(\frac{-\rho\omega_n^{\,2}}{\kappa G}-\frac{\rho\omega_n^{\,2}}{E}+\frac{k}{\kappa AG}+\Gamma_n\right), \tag{16}$$

$$\gamma_n^{\,2} = \frac{1}{2}\left(\frac{-\rho\omega_n^{\,2}}{\kappa G} - \frac{\rho\omega_n^{\,2}}{E} + \frac{k}{\kappa AG} - \Gamma_n \right), \tag{17}$$

$$\beta_n^{\,2} = \frac{\rho\omega_n^{\,2} A - k}{\kappa AG}, \tag{18}$$

$$\Gamma_n = \left[\left(\frac{\rho\omega_n^{\,2}}{\kappa G} + \frac{\rho\omega_n^{\,2}}{E} - \frac{k}{\kappa AG} \right)^2 - \frac{4\rho^2 I\omega_n^{\,4}}{\kappa GEI} + \frac{4\rho A\omega_n^{\,2}}{EI} + \frac{4k\rho I\omega_n^{\,2}}{\kappa AGEI} - \frac{4k}{EI} \right]^{\frac{1}{2}}. \tag{19}$$

For fixed end conditions ($Y_n(0) = Y_n(L) = \Psi_n(0) = \Psi_n(L) = 0$), the lower and upper n-order critical frequencies are determined by the condition for existence of non-zero solution for the following determinant to be solved using Matlab software programming

$$\begin{vmatrix} 1 & 0 \\ \cosh\lambda_n L & \sinh\lambda_n L \\ 0 & \lambda_n + \dfrac{\beta^2}{\lambda_n} \\ \left(\lambda_n + \dfrac{\beta_n^{\,2}}{\lambda_n}\right)\sinh\lambda_n L & \left(\lambda_n + \dfrac{\beta_n^{\,2}}{\lambda_n}\right)\cosh\lambda_n L \end{vmatrix} \tag{20}$$

$$\begin{vmatrix} 1 & 0 \\ \cos\lambda_n L & \sin\lambda_n L \\ 0 & -\left(\dfrac{\beta_n^{\,2}}{\gamma_n} - \gamma_n\right) \\ \left(\dfrac{\beta_n^{\,2}}{\gamma_n} - \gamma_n\right)\sin\gamma_n L & -\left(\dfrac{\beta_n^{\,2}}{\gamma_n} - \gamma_n\right)\cos\gamma_n L \end{vmatrix}_{4\times 4} = 0.$$

3.2.2 Double-elastic beam model

The double-elastic Timoshenko beam model is the most complex but accurate model which considers interlayer radial displacements and the effects of shear deformation and rotary inertia within the DWNT simultaneously. Thus, each of the inner and outer tubes of the DWNTs is modelled as a Timoshenko-elastic beam as follows

$$\begin{aligned}
&-k_1 A_1 G\left[\frac{\partial \Psi_1(x,t)}{\partial x}-\frac{\partial^2 w_1(x,t)}{\partial x^2}\right] \\
&\quad + c\left(w_2(x,t)-w_1(x,t)\right)=\rho A_1 \frac{\partial^2 w_1(x,t)}{\partial t^2}, \\
&EI_1 \frac{\partial^2 \psi_1(x,t)}{\partial x^2} \\
&\quad -k_1 A_1 G\left[\Psi_1(x,t)-\frac{\partial w_1(x,t)}{\partial x}\right]=\rho I_1 \frac{\partial^2 \Psi_1(x,t)}{\partial t^2},
\end{aligned} \tag{21}$$

$$\begin{aligned}
&-k_2 A_2 G\left[\frac{\partial \Psi_2(x,t)}{\partial x}-\frac{\partial^2 w_2(x,t)}{\partial x^2}\right] \\
&\quad + c\left(w_2(x,t)-w_1(x,t)\right)+\left(-k w_2\right)=\rho A_2 \frac{\partial^2 w_2(x,t)}{\partial t^2}, \\
&EI_2 \frac{\partial^2 \psi_2(x,t)}{\partial x^2} \\
&\quad -k_2 A_2 G\left[\Psi_2(x,t)-\frac{\partial w_2(x,t)}{\partial x}\right]=\rho I_2 \frac{\partial^2 \Psi_2(x,t)}{\partial t^2}.
\end{aligned} \tag{22}$$

Here we consider the case in which all nested individual nanotubes have the same fixed end boundary conditions. Thus, it can be obtained that both two nested tubes of an individual DWNT share the same vibrational and

rotational modes. By substituting $w_{1n}(x,t)=W_1 e^{i\omega_n t}Y_n(x)$, $w_{2n}(x,t)=W_2 e^{i\omega_n t}Y_n(x)$, $\Psi_{1n}(x,t)=\psi_1 e^{i\omega_n t}\Psi_n(x)$, and $\Psi_{2n}(x,t)=\psi_2 e^{i\omega_n t}\Psi_n(x)$ into (21) and (22), where $Y_n(x)$ and $\Psi_n(x)$ represent the vibrational and rotational modes of the DWNT and are assumed to be defined by (14) and (15) obtained by single-elastic Timoshenko beam model. The unknown coefficients c_i and frequency determinant are given as follows

$$c_i = \Pi_i c_4 \ , \ i=1,2,3 \tag{23}$$

$$det(\Omega_{\zeta\tau})=0 \ , \ \zeta=1,2 \ , \ \tau=1,2 \tag{24}$$

where

$$\Pi_1=\frac{\dfrac{\gamma_n+\beta_n{}^2/\gamma_n}{\lambda_n+\beta_n{}^2/\lambda_n}sinh\,\lambda_n L+sin\,\gamma_n L}{cos\,\gamma_n L-cosh\,\lambda_n L},$$
$$\Pi_2=\frac{\gamma_n+\beta_n{}^2/\gamma_n}{\lambda_n+\beta_n{}^2/\lambda_n}, \tag{25}$$
$$\Pi_3=-\Pi_1,$$

and

$$\Omega_{11}=EI_1 Y_n{}^4(x)+\left(\frac{\rho^2 EI_1\omega_n{}^2}{\kappa G}+\rho I_1\omega_n{}^2-\frac{EI_1 c}{\kappa A_1 G}\right)Y_n{}''(x)$$
$$+\left(\frac{\rho^2 I_1\omega_n{}^4}{\kappa G}-\rho A_1\omega_n{}^2+c\right)Y_n(x), \tag{26}$$

$$\Omega_{12}=\frac{EI_1 c}{\kappa A_1 G}Y_n{}''(x)+\left(\frac{c\rho I_1\omega_n{}^2}{\kappa A_1 G}-c\right)Y_n(x),$$

$$\Omega_{21} = \frac{EI_2 c}{\kappa A_2 G} Y_n''(x) + \left(\frac{c\rho I_2 \omega_n^{\,2}}{\kappa A_2 G} - c \right) Y_n(x),$$

$$\Omega_{22} = EI_2 Y_n^{\,4}(x) + \left(\frac{\rho^2 EI_2 \omega_n^{\,2}}{\kappa G} + \rho I_2 \omega_n^{\,2} - \frac{EI_2 c}{\kappa A_2 G} - \frac{kEI_2}{\kappa A_2 G} \right) Y_n''(x)$$
$$+ \left(\frac{\rho^2 I_2 \omega_n^{\,4}}{\kappa G} - \rho A_2 \omega_n^{\,2} - \frac{c\rho I_2 \omega_n^{\,2}}{\kappa A_2 G} - \frac{k'\rho I_2 \omega_n^{\,2}}{\kappa A_2 G} + k + c \right) Y_n(x).$$

Furthermore for the first three vibrational bending modes of a DWNT fiber, an auxiliary condition can be defined as follows

$$\begin{aligned} \psi_n\left(\frac{L}{2}\right) &= 0 \text{ , for the first and third mode} \\ Y_n\left(\frac{L}{2}\right) &= 0 \text{ , for the second mode} \end{aligned} \tag{27}$$

ω_n , λ_n and γ_n can be obtained by considering (20), (24) and (27) simultaneously to be solved using Matlab software programming.

4. Numerical Simulation and Discussion

In order to investigate the effects of matrix stiffness, nanotube length and chirality on the selection of the appropriate method for the frequency analysis of carbon nanotube fibers embedded in composite materials (see Fig. 1), all above mentioned theories were applied to three different DWNTs, (5,5)/(10,10), (5,5)/(17,0) and (5,5)/(15,4), with the inner and outer diameters $d_i = 0.68\,\text{nm}$ and $d_o = 1.36\,\text{nm}$, respectively. In this section, these different models are compared and the lower and upper n-

order critical frequencies are shown for different aspect ratios (L/d), mode numbers (n) and matrix stiffness (k) in Figs. (2) and (3).

When the matrix spring constant k is much smaller than the intertube interaction coefficient c (i.e., $k/c = 0.001$), the lower n-order resonant frequency given by non-coaxial Timoshenko theory ω_{LDT} is close to the resonant frequency given by coaxial Timoshenko beam model ω_{ST}. The relative error is less than 3% for n=1 and less than 15% for n=3. In this case, the lower n-order Timoshenko resonant frequency ω_{LDT} can be estimated by coaxial Timoshenko beam model but on the other hand, the higher n-order intertube Timoshenko and Euler-Bernoulli resonant frequency which is always above 13 THz, and thus much higher than the lower n-order resonant frequency, should be obtained by non-coaxial Timoshenko beam model (see Figs. (2) and (3)).

However, as the ratio k/c increases and approaches 1, the ratio of the higher n-order intertube resonant frequency to the frequency given by single Euler-Bernoulli beam model will drastically decrease and the lower n-order resonant frequencies predicted by single and double Timoshenko beam models move towards the Euler-Bernoulli beam model prediction results (see Figs. (2) and (3)). In this case the lower n-order resonant frequency can be estimated by coaxial Euler-Bernoulli beam model for the lower mode numbers (i.e. n=1,2), while for the higher modes (i.e. n=3), the

DWNTs does not keep their otherwise concentric structure and non-coaxial Euler-Bernoulli beam should be considered to improve the accuracy and reliability of the results. On the other hand, for the higher *n*-order intertube resonant frequencies, the resonant frequencies predicted by Timoshenko beam models move towards those of Euler-Bernoulli beam model only for DWNTs of lower aspect ratio (i.e. $L/d = 10$). For the prediction of higher aspect ratio DWNT fragments (i.e. $L/d = 50$), non-coaxial Timoshenko beam models should be considered to obtain more reliable frequency results.

By more increasing the ratio k/c to 100, when $L/d = 10$, the ratios of the higher n-order resonant frequencies for both Euler-Bernoulli and Timoshenko double beam models to the single Euler beam model converges to 1.21 for all three modes which denotes that the single Euler beam model predicts the higher *n*-order resonant frequency instead of the lower one and it is anticipated that this certain number is mainly determined by the aspect ratio L/d of the DWNTs. The lower *n*-order resonant frequency for Euler-Bernoulli and Timoshenko double beam models tends to 2.93THz and 2.83THz when *n*=1, and to 3.03THz and 2.87THz when *n*=2, and to 3.31 THz and 3.18 THz when *n*=3, respectively. It can be seen that the lower *n*-order resonant frequency given by Timoshenko and Euler-Bernoulli beam models are in a good agreement

with each other. While, both are nearly about one order of magnitude smaller than the frequency ω_{SE} given by the single Euler beam model. Therefore, when the stiffness of the matrix is high enough (i.e. $k/c = 100$), non-coaxial Euler beam model can reasonably predict the lower *n*-order resonant frequencies and mode shapes of a DWNT fiber.

As it can be seen from Figs. (2) and (3), the molecular dynamics frequency analysis results of three different DWNTs, (5,5)/(10,10), (5,5)/(17,0) and (5,5)/(15,4) having different outer tube chiralities but the same diameter, is almost compatible with each other and also with the results of continuum theory, which clarify that the effects of chiralities on frequency analysis of DWNTs are negligible.

Table 1 shows the effect of matrix stiffness on appropriate carbon nanotube embedded composites frequency analysis theories for different ratios k/c and L/d.

5. Conclusion

The effects of the matrix stiffness, nanotube length and chirality on the resonant frequencies of DWNT fibers were studied by considering MD simulations and four different elastic models namely, Timoshenko and Euler-Bernoulli beam models and for both coaxial and non-coaxial assumptions. The effects of shear deformation, rotary inertia and

concentricity of the tubes on the accuracy and reliability of the DWNT fibers frequency analysis results were determined. It was found that for soft matrixes (i.e., $k/c \approx 0.001$), the lower n-order Timoshenko resonant frequency ω_{LDT} can be estimated by coaxial Timoshenko beam model but on the other hand, the higher n-order resonant frequency should be obtained by non-coaxial Timoshenko beam model. However, for hard matrixes (i.e., $k/c \approx 1$), the lower n-order resonant frequencies predicted by single and double Timoshenko beam models move towards the Euler-Bernoulli beam model prediction results and can be estimated by coaxial Euler-Bernoulli beam model for the lower mode numbers (i.e. n=1,2) and non-coaxial Euler-Bernoulli beam model for the higher modes (i.e. n=3). For the prediction of higher n-order resonant frequencies, non-coaxial Timoshenko beam models should be considered to obtain more reliable frequency results. When using extremely hard matrixes (i.e., $k/c \approx 100$), non-coaxial Euler beam model can reasonably predict the lower n-order resonant frequencies of a DWNT fiber. Molecular dynamics frequency analysis results of three different DWNTs, (5,5)/(10,10), (5,5)/(17,0) and (5,5)/(15,4) denotes that the effects of chiralities on frequency analysis of DWNTs are negligible.

References

1. Bachtold, A., Hadley, P., Nakanishi, T. and Dekker, C., "Logic circuits with carbon nanotube transistors," Science, 294, pp.1317–1320 (2001).
2. Derycke, V., Martel, R., Appenzeller, J. and Avouris, P., "Carbon nanotube inter- and intramolecular logic gates," Nanoletters, 1, pp.453–456 (2001).
3. Lusti, H. R. and Gusev, A. A., "Finite element predictions for the thermoelastic properties of nanotube reinforced polymers," Model Simulat. Mater. Sci. Eng., 12(3), pp.107–119 (2004).
4. Lau, K. T. and Hui, H., "The revolutionary creation of new advanced materials—carbon nanotube," Composite B, 33, pp.263–277 (2003).
5. Wong, E. W., Sheehan, P. E. and Lieber, C. M., "Nanobeam mechanics: elasticity, strength, and toughness of nanorods and nanotubes," Science, 277, pp.1971–1975 (1997).
6. Falvo, M. R., Clary, G. J., Taylor, R. M., Chi, V., Brooks, F. P. and Washburn, S., "Bending and buckling of carbon nanotubes under large strain," Nature, 389, pp.582–584 (1997).
7. Xiaohu, Y. and Qiang, H., "Torsional Buckling and Postbuckling Equilibrium Path of Double-Walled Carbon Nanotubes," Compos. Sci. Technol., DOI 10.1016/j.compscitech.2007.05.025.

8. Wang, Q., Quek, S. and Varadan, V., “Torsional buckling of carbon nanotubes,” Physics Letters A, 367, pp.135–139 (2007).
9. Treacy, M., Ebbesen, T., Gibson, J., “Exceptionally high young’s modulus observed for individual carbon nanotubes,” Nature, 381, pp.678–680 (1996).
10. Guoxin, C., Xi, C. and Kysar, W., “Thermal vibration and apparent thermal contraction of single-walled carbon nanotubes,” J. Mech. Phys. Solids, 54, pp.1206-1236 (2006).
11. Yoon, J., Ru, C. and Mioduchowski, A., “Vibration of an embedded multiwall carbon nanotube,” Compos. Sci. Technol., 63, pp.1533-1542 (2003).
12. Sun, C. and Liu, K., “Vibration of multi-walled carbon nanotubes with initial axial loading,” Solid State Communications, 143, pp.202–207 (2007).
13. Wang, X. and Cai, H., “Effects of initial stress on non-coaxial resonance of multi-wall carbon nanotubes,” Acta. Materialia, 54, pp.2067-2074 (2006).
14. Yoon, J., Ru, C. and Mioduchowski, A., “Vibration and instability of carbon nanotubes conveying fluid,” Compos. Sci. Technol., 65, pp.1326-1336 (2005).

15. Ahlers, F., Fletcher, N., Ebbecke, J. and Janssen, B., "Surface acoustic wave driven quantized current transport," Curr. Appl. Phys., 4, pp.529-533 (2004).
16. Smith, B. and Luzzi, D., "Formation mechanism of fullerene peapods and coaxial tubes: a path for large scale synthesis," Chem. Phys. Lett., 321, pp.169–174 (2000).
17. Bandow, S., Takizawa, M., Hirahara, K., Yudasaka, M. and Iijima, S., "Raman scattering study of double-wall carbon nanotubes derived from the chains of fullerenes in single-wall carbon nanotubes," Chem. Phys. Lett., 337, pp.48–54 (2001).
18. Thostenson, E., Li, W., Wang, D., Ren, Z. and Chou, T., "Carbon nanotube/carbon fibers hybrid multiscale composites," Appl. Phys. Lett., 91, pp.6034–6036 (2002).
19. Rueckers, T., Kim, K., Joselevich, E., Tseng, G., Cheung, C. and Lieber, C., "Carbon nanotube-based nonvolatile random access memory for molecular computing," Science, 289, pp.94–97 (2000).
20. Cumings, J. and Zettel, A., "Low-friction nanoscale linear bearing realized from multiwall carbon nanotubes," Science, 289, pp.602–604 (2000).
21. Zheng, Q. and Jiang, Q., "Multiwalled Carbon Nanotubes as Gigahertz Oscillators," Phys. Rev. Lett., 88, pp. 045503-1-045503-3 (2002).

22. Legoas, S. B., Coluci, V. R., Braga, S. F., Coura, P. Z., Dantas S. O. and Galva, D. S., " Molecular-Dynamics Simulations of Carbon Nanotubes as Gigahertz Oscillators," Phys. Rev. Lett., 90, pp. 055504-1-055504-4 (2003).
23. Brenner, D. W., "Empirical potential for hydrocarbons for use in simulating the chemical vapor deposition of diamond films," Phys. Rev. B, 42, pp. 9458-9471 (1990).
24. Girifalco, L. A., Hodak, M. and Lee R. S., "Carbon nanotubes, buckyballs, ropes, and a universal graphitic potential," Phys. Rev. B, 62, pp. 13104-13110 (2000).
25. Lanir, Y. and Fung, Y., "Fiber composite columns under compressions," J. Compos. Mater., 6, pp.387–401 (1972).
26. Hahn, H. and Williams, J., "Compression failure mechanisms in unidirectional composites," Composite Materials: Testing and Design, 7, pp.115–139 (1984).
27. Lourie, O., Cox, D. and Wagner, H., "Buckling and collapse of embedded carbon nanotubes," Phys. Rev. Lett., 81, pp.1638–1641 (1998).
28. Kasumov, A., Bouchiat, H., Reulet, B., Stephan, O., Khodos, I. and Gorbatov, Y., "Conductivity and atomic structure of isolated multiwalled carbon nanotubes," Europhysics Letters, 43, pp.89–94 (1998).

29. Cowper, G., “The shear coefficient in timoshenko’s beam theory,” J. Appl. Mech. ASME, 12, pp.335-340 (1966).

Table 1

Table 1- The effects of matrix stiffness (k/c) and carbon nanotubes aspect ratio (L/d) on appropriate carbon nanotube embedded frequency analysis theory.

	k/c	$L/d=10$	$L/d=50$
Lower n-order resonant frequency	<0.01	Coaxial Timoshenko	Coaxial Timoshenko
	<1	Coaxial Euler*	Coaxial Euler
	>>1	Non-coaxial Euler	Non-coaxial Euler
Higher n-order resonant frequency	<0.01	Non-coaxial Timoshenko	Non-coaxial Timoshenko
	>0.01	Non-coaxial Euler	Non-coaxial Timoshenko

* Non-coaxial Euler theory should be used when n=3.

Fig. 1- Double-walled CNT model embedded in an elastic matrix by a spring constant *k*.

Fig. 2- Molecular dynamics and continuum analysis of (5,5)/(10,10), (5,5)/(17,0) and (5,5)/(15,4) DWNTs owning aspect ratio $L/d = 10$ against the matrix stiffness (*k*), for different mode numbers (a) first mode (*n*=1), (b) second mode (*n*=2) and, (c) third mode (*n*=3).

Fig. 3- Molecular dynamics and continuum analysis of (5,5)/(10,10), (5,5)/(17,0) and (5,5)/(15,4) DWNTs owning aspect ratio $L/d = 50$ against the matrix stiffness (*k*), for different mode numbers (a) first mode (*n*=1), (b) second mode (*n*=2) and, (c) third mode (*n*=3).

Fig. 1

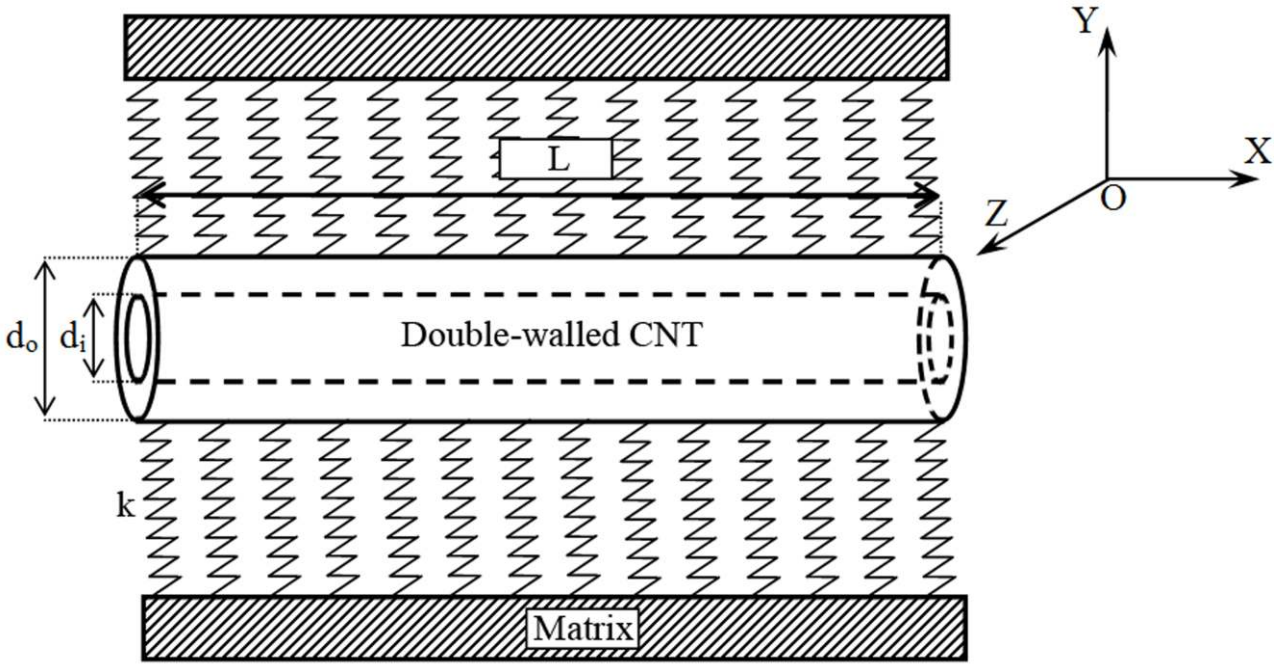

Fig. 1

Fig. 2a

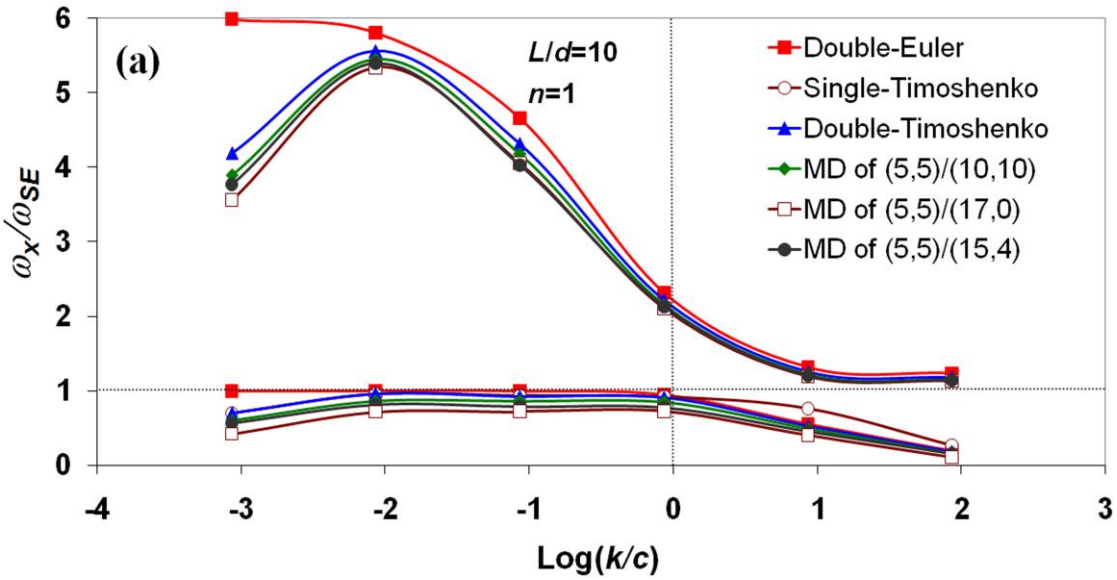
(a)
L/d=10
n=1
Double-Euler
Single-Timoshenko
Double-Timoshenko
MD of (5,5)/(10,10)
MD of (5,5)/(17,0)
MD of (5,5)/(15,4)
ωx/ωSE
Log(k/c)
6
5
4
3
2
1
0
-4
-3
-2
-1
0
1
2
3

Fig. 2a

Fig. 2b

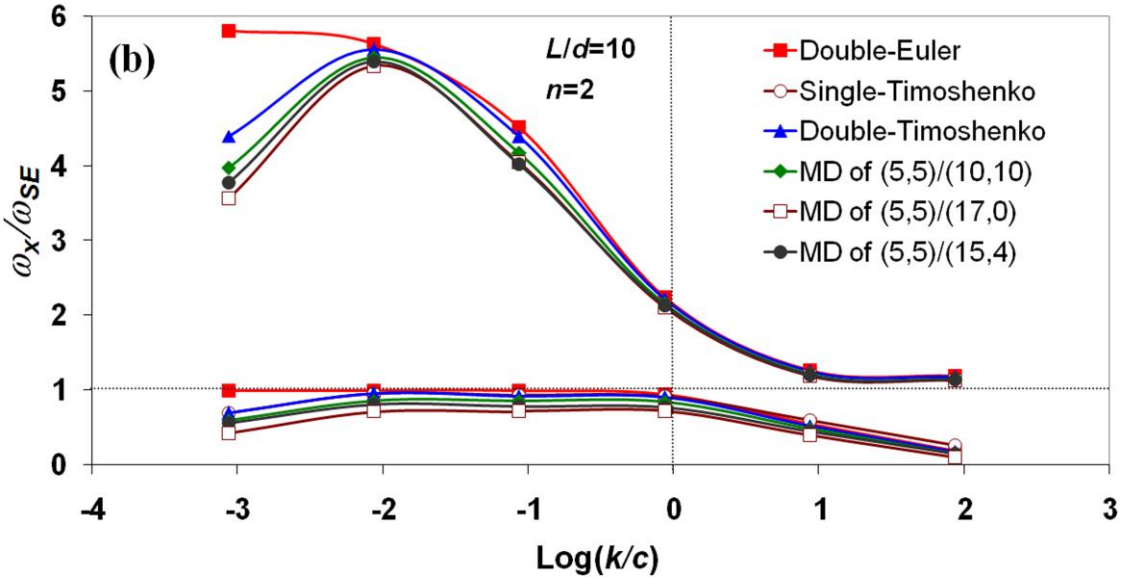
(b)
L/d=10
n=2
Double-Euler
Single-Timoshenko
Double-Timoshenko
MD of (5,5)/(10,10)
MD of (5,5)/(17,0)
MD of (5,5)/(15,4)
ω_x/ω_SE
Log(k/c)
6
5
4
3
2
1
0
-4
-3
-2
-1
0
1
2
3

Fig. 2b

Fig. 2c

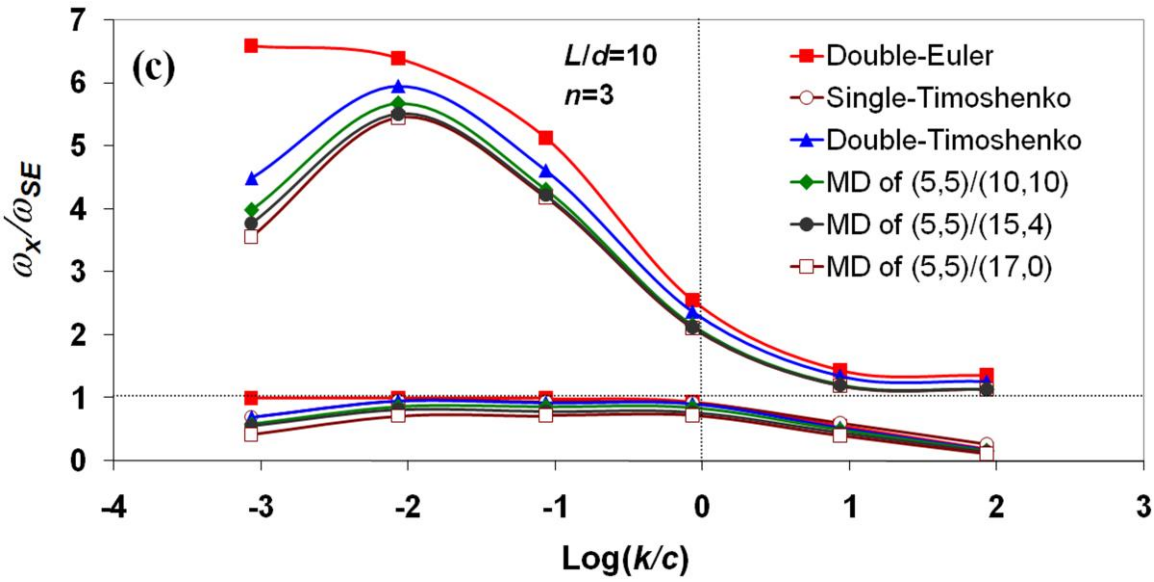
(c)
L/d=10
n=3
Double-Euler
Single-Timoshenko
Double-Timoshenko
MD of (5,5)/(10,10)
MD of (5,5)/(15,4)
MD of (5,5)/(17,0)
ω_x/ω_SE
Log(k/c)
7
6
5
4
3
2
1
0
-4
-3
-2
-1
0
1
2
3

Fig. 2c

Fig. 3a

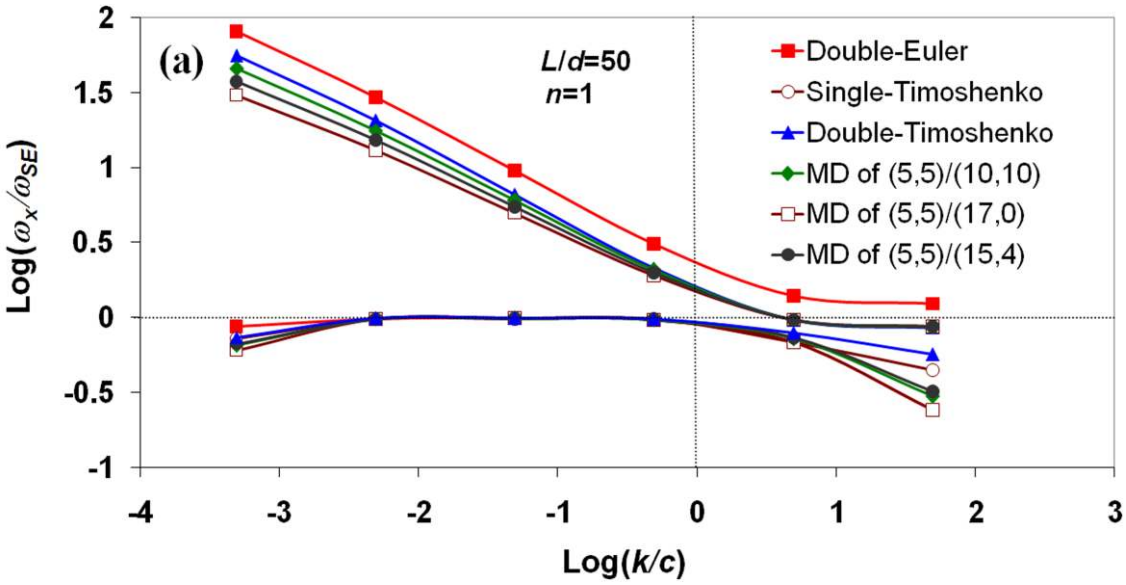
(a)
L/d=50
n=1
Double-Euler
Single-Timoshenko
Double-Timoshenko
MD of (5,5)/(10,10)
MD of (5,5)/(17,0)
MD of (5,5)/(15,4)
Log(ωx/ωSE)
Log(k/c)
2
1.5
1
0.5
0
-0.5
-1
-4
-3
-2
-1
0
1
2
3

Fig. 3a

Fig. 3b

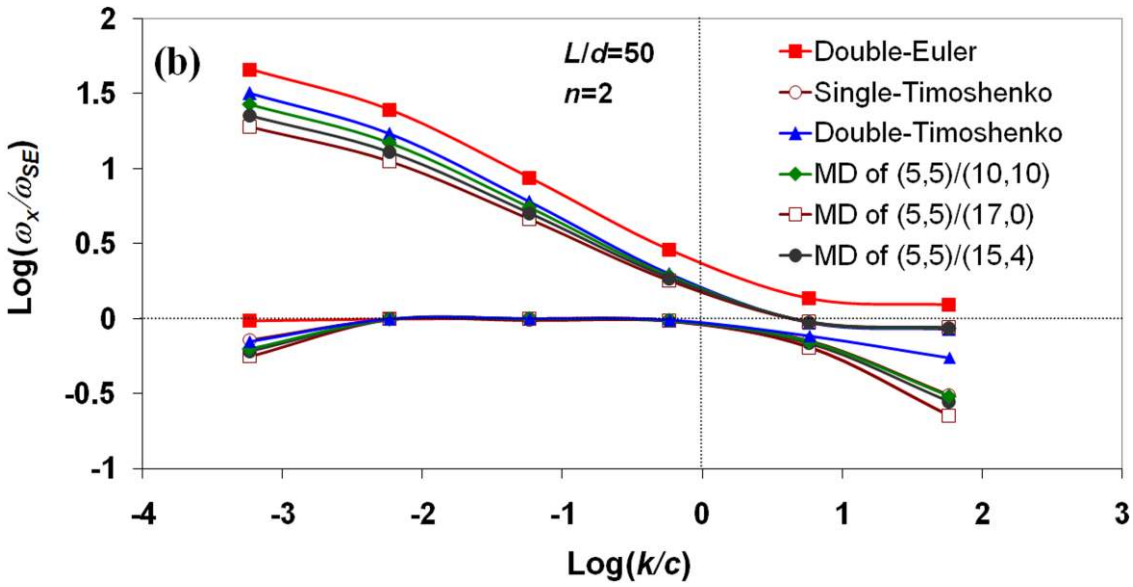
(b)
L/d=50
n=2
Double-Euler
Single-Timoshenko
Double-Timoshenko
MD of (5,5)/(10,10)
MD of (5,5)/(17,0)
MD of (5,5)/(15,4)
Log(ωx/ωSE)
Log(k/c)
2
1.5
1
0.5
0
-0.5
-1
-4
-3
-2
-1
0
1
2
3

Fig. 3b

Fig. 3c

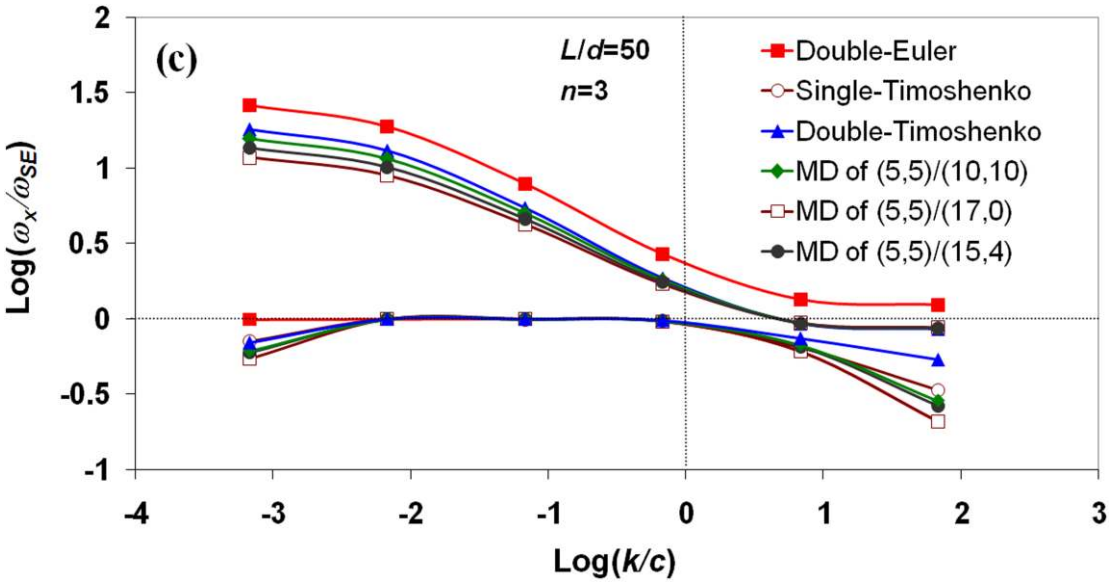
(c)
L/d=50
n=3
Double-Euler
Single-Timoshenko
Double-Timoshenko
MD of (5,5)/(10,10)
MD of (5,5)/(17,0)
MD of (5,5)/(15,4)
Log(ω_x/ω_SE)
Log(k/c)
2
1.5
1
0.5
0
-0.5
-1
-4
-3
-2
-1
0
1
2
3

Fig. 3c